Magnetic Dephasing in Mesoscopic Spin Glasses

Thibaut Capron,[1] Guillaume Forestier,[1] Angela Perrat-Mabilon,[2] Christophe Peaucelle,[2] Tristan Meunier,[1] Christopher Bäuerle,[1] Laurent P. Lévy,[1,4,5] David Carpentier,[3] and Laurent Saminadayar[1,4,5,*]

[1]*CNRS, Institut Néel, B.P. 166, 38042 Grenoble Cedex 09, France*
[2]*Institut de Physique Nucléaire de Lyon, Université de Lyon, Université de Lyon 1, CNRS & IN2P3, 04 rue Enrico Fermi, 69622 Villeurbanne Cedex, France*
[3]*Laboratoire de Physique, École Normale Supérieure de Lyon, 47 allée d'Italie, 69007 Lyon, France*
[4]*Institut Néel, Université Grenoble Alpes, B.P. 53, 38041 Grenoble Cedex 09, France*
[5]*Institut Universitaire de France, 103 boulevard Saint-Michel, 75005 Paris, France*

(Received 2 April 2013; published 31 October 2013)

We have measured universal conductance fluctuations in the metallic spin glass Ag:Mn as a function of temperature and magnetic field. From this measurement, we can access the phase coherence time of the electrons in the spin glass. We show that this phase coherence time increases with both the inverse of the temperature and the magnetic field. From this, we deduce that decoherence mechanisms are still active even deep in the spin glass phase.

DOI: 10.1103/PhysRevLett.111.187203 PACS numbers: 75.50.Lk, 73.23.−b, 73.40.−c, 75.20.Hr

Spin glasses are one of the most fascinating states of matter. It has attracted the interest of a large community for several decades, as it is one of the most fundamental problems in condensed matter physics [1]. Spin glass appears when magnetic atoms are randomly diluted in a nonmagnetic metallic host. As the spatial distribution is random, so are the Ruderman-Kittel-Kasuya-Yoshida (RKKY) interactions between the spins. This leads to a frustration between the magnetic moments and their couplings. It is this interplay between disorder and frustration that leads to the formation of a *spin glass* below a transition temperature T_{sg}. The very nature of the ground state is still heavily debated and may consist in an unconventional state of matter with remarkable behavior [2]. Transport properties of these metallic spin glasses, however, have not been studied thoroughly. In particular, only very few studies, experimental or theoretical, have addressed the question of the quantum coherence of the electrons in a metallic spin glass, and it is usually taken for granted that, as spins are frozen, inelastic scattering processes due to spins are also frozen and one should recover the coherence time observed in a Fermi liquid.

It has been widely recognized that transport measurement can be a powerful tool to probe the quantum coherence in metallic systems [3] and that this concept can be extended to spin glasses [4]. Recently, the interest in quantum transport measurements in spin glasses has been even renewed, thanks to the idea that this type of measurement could give access to the structure of the ground state of the system [5].

In this Letter, we present measurements of universal conductance fluctuations (UCFs) in a metallic spin glass as a function of temperature and magnetic field. From this, we deduce the phase coherence time of the electrons; we show it increases as the temperature decreases, in agreement with theoretical predictions. Moreover, from the magnetic field dependence of the decoherence rate, we show that decoherence mechanisms persist deep in the spin glass phase.

Samples have been fabricated on a silicon–silicon-oxide wafer using standard electron-beam lithography on a polymethylmethacrylate resist. Geometry of the sample consists in a long (length $L \approx 2\ \mu$m) and thin (width $w \approx 50$ nm, thickness $t \approx 40$ nm) wire (see the inset of Fig. 1). Several contacts have been put along the wire, in order to measure the resistance over different lengths and to thermalize properly the electrons along the wire. Silver has been evaporated using a dedicated electron gun evaporator and a 99.9999% purity source without an adhesion layer. Electronic properties of pure samples fabricated during the same run have been measured in previous works

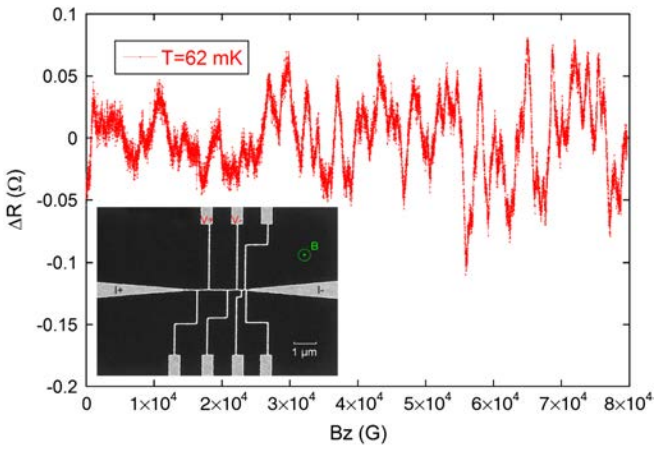

FIG. 1 (color online). Magnetoresistance of a spin glass Ag sample implanted with 700 ppm of manganese. The magnetic field is applied perpendicularly to the sample. Inset: Scanning electron microscopy of the sample; current and voltage probes are indicated in red.

[6,7], leading to the values $l_e = 43$ nm for the elastic mean free path, $\rho = 2.15\ \mu\Omega \cdot$ cm for the resistivity, and $L_\phi = 7\ \mu$m for the phase coherence length at low temperature (below ≈ 50 mK). Samples have then been implanted with Mn^{2+} ions of energy 70 keV. The energy has been chosen after numerical simulations based on the SRIM software in order to ensure that ions will end up in the sample following a Gaussian distribution whose maximum lies in the middle of the sample thickness. Moreover, this technique of implantation allows us to avoid clustering or migration of the Mn^{2+} ions, as no further annealing has been performed on the samples; moreover, it has been shown that this technique does not change the intrinsic properties of the metal [7]. The ion dose, measured via the current of the implanter, has been chosen in order to give a final ion concentration in the wire of 700 ppm; such a concentration leads to a transition temperature of $T_{sg} \approx 700$ mK [8,9], as has been demonstrated recently by transport measurements [10]: it is thus easy to perform measurements well below T_{sg}. The sample has been cooled down in a dilution fridge whose base temperature T is ≈ 50 mK and equipped with a superconducting coil of maximum magnetic field $B = 8$ T. Transport measurements have been carried out using an ac lock-in technique at a frequency of 11 Hz in a bridge configuration and using a very low current of 250 nA, in order to avoid any overheating of the sample. Signal is amplified using an ultralow noise homemade voltage amplifier (voltage noise $S_v = 500\ \mathrm{pV}/\sqrt{\mathrm{Hz}}$) at room temperature. All the measuring lines connecting the sample to the experimental setup consist in lossy coaxes which ensure a very efficient radio-frequency filtering and thus a good thermalization of the sample [11–13]. At 4.2 K, the resistance of our sample is $R \approx 10\ \Omega$.

Universal conductance fluctuations are obtained by measuring the magnetoresistance of the sample between 0 and 8 T. The field is swept at a rate of 20 mG/s in order to avoid excessive eddy currents heating of the fridge. After subtraction of the classical magnetoresistance of a spin glass [14–16], one clearly sees the UCFs, as shown in Fig. 1. These magnetoresistance traces are decorrelated by a temperature cycling well over T_{sg}, signaling the coupling of this magnetoresistance to the frozen spins. On the other hand, it should be stressed that they are completely reproducible over the sweeping direction. Moreover, we observe that the maximum magnetic field applied is much larger than the expected critical field $B \gg B_c = k_B T_{sg}/\mu_B$, with μ_B the Bohr magneton and k_B the Boltzmann constant. Such a result is similar to what has been observed in the work of Lévy *et al.* on a Cu:Mn system [4]: the exact spin configuration of a spin glass is preserved after a magnetic cycling to a very high magnetic field at a temperature of $\approx T_{sg}/10$. Within the mean-field phase diagram of spin glasses, two critical lines exist related to the freezing of the longitudinal component (the "de Almeida–Thouless" line) and the transverse component of the spins (the "Gabay-Toulouse" line). While magnetization measurements usually probe the longitudinal freezing and observe a freezing field of the order of B_c, transport measurements are sensitive to the freezing of both components of the spins. Similarly, this transverse freezing has also been probed in torque experiments, as reported in Ref. [17]. Remarkably, both experiments signal a much stronger freezing field than the expected B_c. These measurements appear consistent with the numerical result of Imagawa and Kawamura (see Fig. 20 in Ref. [18]); other scenarios [1,2] should be reconsidered in light of this experiment.

We now consider the *amplitude* of these UCFs as a function of the magnetic field; for this purpose, we have plotted in Fig. 2 the peak-to-peak amplitude (extracted from the inset of the figure) as a function of the magnetic field. Two regimes are clearly visible: a low-field regime (typically below $B \lesssim 2.5$ T) and a high-field regime ($B \gtrsim 4.5$ T). They differ by the amplitude of the UCFs, which is 5 times larger in the high-field regime. Such an increase of the amplitude of the UCFs manifests an increase of the phase coherence length of the electrons L_ϕ [19]. More precisely, as long as L_ϕ is smaller than both the system length and the thermal length $L_T = \sqrt{\hbar D/k_B T}$, with D the diffusion coefficient and T the temperature, $L_\phi \leq L_T, L$, the amplitude of the UCFs scales as $\Delta G_{\mathrm{UCFs}} \propto (L_\phi/L)^{3/2}$. In this regime, an increase of the UCF manifests the corresponding increase of the phase coherence length. On the other hand, for $L_T \leq L_\phi \leq L$, the UCF amplitude saturates to $\Delta G_{\mathrm{UCFs}} \propto (L_T/L)$ and becomes independent of L_ϕ. The results of Fig. 2 are thus interpreted as an increase of the phase coherence length until it reaches the thermal length $L_\phi \simeq L_T$ for $B \simeq 4.5$ T.

We will relate this increase of the phase coherence length to a change of magnetic dephasing due to the polarization of the ensemble of magnetic impurities.

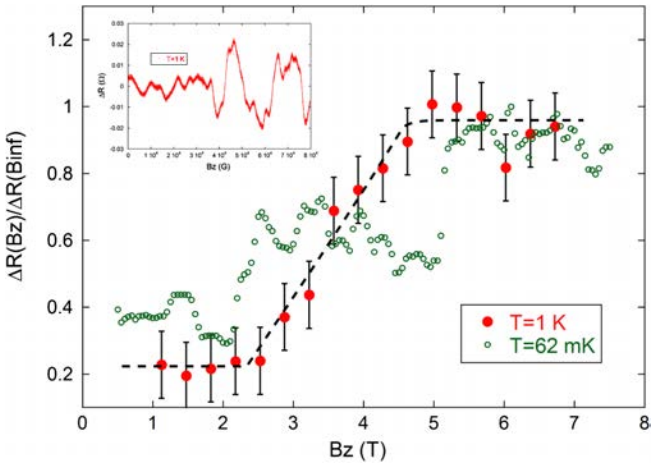

FIG. 2 (color online). Relative amplitude of the universal conductance fluctuations as a function of the magnetic field. The inset shows that this increase is already clear on the direct magnetoresistance trace.

The scale in magnetic field on which this polarization occurs is governed by the typical amplitude J_{RKKY} of the couplings between impurity spins. The magnetization of Cu:Mn bulk spin glass with an Mn concentration in the range 1%–10% in a high field up to 40 T shows a progressive saturation with field [20]. Rescaling these data by the impurity concentration, we infer a characteristic field of 2.5 T for our 700 ppm Ag:Mn sample, compatible with the data represented in Fig. 2. We now focus on the low- and intermediate-field regimes. For the range of parameters explored here, the electron-phonon and electron-electron mechanisms are subdominant and the dephasing rate $1/\tau_\phi$ is dominated by the electron-magnetic impurities processes [21] $1/\tau_\phi \simeq 1/\tau_{e-s}$. We thus focus on the magnetic dephasing rate and its evolution with magnetic field and temperature. We account for the strong couplings between the magnetic impurities through an effective field description [22]. In this description, the spin $\vec{S}_i$ of each magnetic impurity is submitted to a effective magnetic field $\vec{h}_i$ originating from both the competing RKKY couplings to the neighboring spins and from the external magnetic field $\vec{B}$. At each temperature and magnetic field, the spin glass state is thus described by a distribution of effective fields $P_{T,\vec{B}}(\vec{h}_i)$ over the various impurities. Each impurity is thus treated independently of the others. The corresponding magnetic dephasing can be described using the Kondo dephasing mechanism [23,24]. Two different dephasing mechanisms occur, depending on the strength of the effective field $|\vec{h}_i|$. (i) For the effective "free spins," of concentration $n_{\mathrm{imp}}^{\mathrm{free}}$ and for which $g\mu_B|\vec{h}_i| \leq kT$, the dominant dephasing mechanism is the usual Kondo dephasing [23,24] with a rate [25]

$$\frac{1}{\tau_{e-s}^{\mathrm{free}}} = \frac{8\pi n_{\mathrm{imp}}^{\mathrm{free}}}{\rho(E_F)} \frac{S(S+1)}{\ln^2 T/T_K}, \tag{1}$$

with $\rho(E_F)$ the density of states at the Fermi energy, S the spin of the impurities, T_K the Kondo temperature of the alloy, and $n_{\mathrm{imp}}^{\mathrm{free}}$ related to the total concentration of impurities by

$$n_{\mathrm{imp}}^{\mathrm{free}} \simeq n_{\mathrm{imp}} P_{T,B}(h=0) \frac{k_B T}{g\mu_B}. \tag{2}$$

(ii) For the other spins (such that $g\mu_B|\vec{h}_i| \geq kT$), the dephasing occurs via a different virtual process mechanism with a rate [see Eq. (7) in Ref. [25]]

$$\frac{1}{\tau_{e-s}^{\mathrm{pol}}} \propto \frac{1}{B^2}. \tag{3}$$

Note that this virtual process is much less efficient than the direct process described in Eq. (1).

When both are present, virtual processes are thus negligible: this corresponds to the low-field regime of Fig. 2. The plateau of ΔR in this regime hints that the probability $P_{T,B}(h=0)$ varies slowly over this magnetic field range. The change of behavior at $B \simeq 2.5$ T indicates the disappearance of the direct Kondo dephasing. Beyond this field, most of the impurities contribute to the dephasing through the virtual process mechanism [Eq. (2)]. In this regime, τ_ϕ is proportional to B^2 [Eq. (3)], leading to an amplitude of the UCFs scaling as $\Delta R \propto L_\phi^{3/2} \propto B^{3/2}$, in good agreement with our experimental data (Fig. 2).

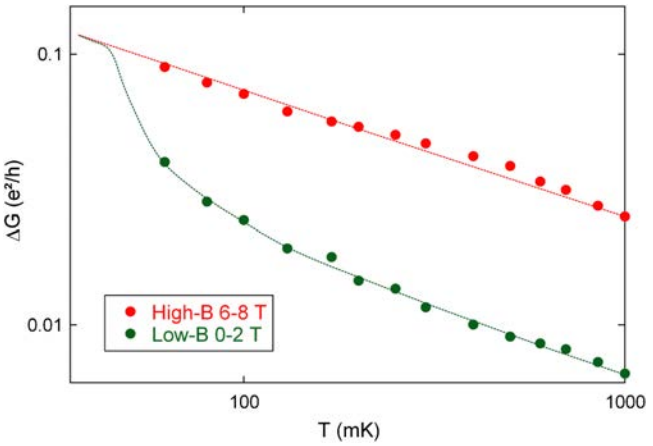

FIG. 3 (color online). Amplitude of the UCFs as a function of temperature, for high field ($B \geq 6$ T) and low field ($B \leq 2$ T). Note that the "high-field" curve follows nicely a power law, whereas the "low-field" curve tends to join it at very low temperature. The dotted lines are guides for the eyes.

In Fig. 3, we have plotted the amplitude of the UCFs for both high and low magnetic field, as a function of temperature. The high-field ($B \geq 6$ T) amplitude is found to scale as $\Delta G_{\mathrm{UCFs}} \propto T^{-1/2}$. This scaling is compatible with our previous analysis using $L_T = (\hbar D/T)^{1/2} \simeq T^{-1/2}$. To analyze quantitatively the low-field regime ($B \leq 2$ T), we extract the phase coherence rate τ_ϕ from the amplitude of the UCFs and then subtract the Altshuler-Aronov-Khmelnitsky contribution [26]: this provides the (dominant) magnetic dephasing rate. Its temperature dependence is depicted in Fig. 4. Using Eq. (1), we can then extract the temperature

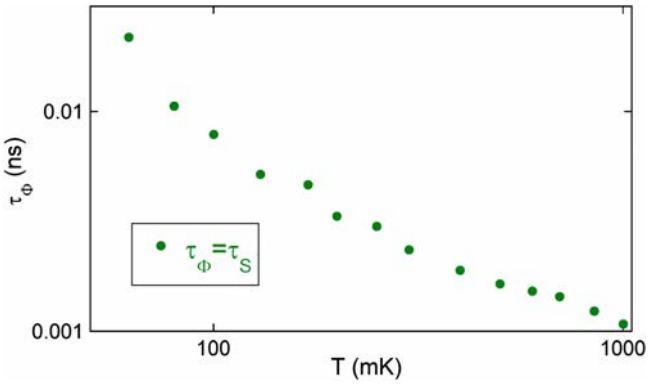

FIG. 4 (color online). Decoherence rate as a function of temperature extracted from the low-field curve of Fig. 3.

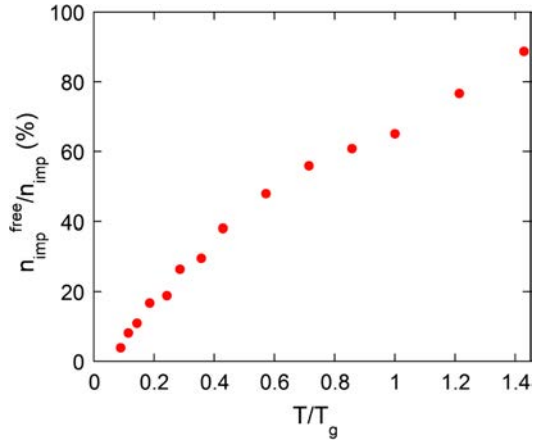

FIG. 5 (color online). Fraction of free spins (normalized to the initial concentration of magnetic impurities) as a function of the normalized temperature (normalized to the freezing temperature T_{sg}).

dependance of the fraction of free spins n_{imp}^{free}/n_{imp}: the result is shown in Fig. 5. Note, however, that above 1 K, the data are not reliable, as the (neglected) electron-phonon scattering starts to play a non-negligible role in the decoherence processes. The obtained temperature dependance is compatible with $n_{imp}^{free}/n_{imp} \propto T^{\alpha}$, with α close to 1. Note that this leads to a magnetic susceptibility $\propto n_{imp}^{free} \times 1/T \simeq Cste$, in agreement with experimental data. We can then extract the temperature scaling behavior of the probability $P_{T,B}(h_i = 0) \propto T^{\alpha-1}$ using Eq. (2). The experimental data are compatible with either a constant probability ($\alpha = 1$) or a weak pseudogap behavior ($\alpha \geq 1$) [22].

What can we infer from these measurements? In our system, both the implantation concentration as well as the remanent effect indicate a freezing temperature of ≈ 700 mK [10]. It is commonly believed that slightly below T_{sg}, (almost) all the spins are completely frozen. Mesoscopic probes, which have so far not been exploited in the field of spin glasses, demonstrate that this is actually not the case: even at low temperature (one-tenth of T_{sg}), almost 10% of the spins are still free to flip by thermal activation. This shows that the spin glass transition is indeed very broad, a total freezing of all the spins appearing only below $T_{sg}/10$. Moreover, even at low temperature and below the characteristic field B_c, a finite fraction of the spins remains actually free.

To conclude, we have measured phase coherent transport in an Ag:Mn spin glass doped at a level of 700 ppm. We have shown that the universal conductance fluctuations are perfectly reproducible up to a field of 8 T, i.e., a field much larger than the characteristic field $B_c \approx k_B T_{sg}/\mu_B$. Moreover, we observe a strong increase of the amplitude of these UCFs above a field of 2.5 T; this increase is interpreted as an increase of the phase coherence length due to the polarization of the spins. Finally, we describe the gradual freezing of the spins when lowering the temperature. This constitutes the first experimental probe of the fraction of free spins in a spin glass. This study paves the way for a measurement of the overlaps between microscopic spin configurations in the spin glass phase [27].

We are indebted to H. Pothier and H. Bouchiat for the use of their Joule evaporators. We thank L. Glazman, G. Paulin, E. Orignac, B. Spivak, H. Bouchiat, É. Vincent, D. Estève, A. Rosch, T. Micklitz, R. Whitney, and H. Alloul for fruitful discussions. This work has been supported by the French National Agency (ANR) in the frame of its "Programmes Blancs" (MESOGLASS Project).

*laurent.saminadayar@neel.cnrs.fr

[1] *Complex Systems*, *Proceedings of the Les Houches Summer School, Session No. LLXXXV*, edited by J.-P. Bouchaud, M. Mézard, and J. Dalibard (Springer-Verlag, Berlin, 2006).
[2] É. Vincent, J. Hammann, and M. Ocio, J. Stat. Phys. **135**, 1105 (2009).
[3] F. Schopfer, C. Bauerle, W. Rabaud, and L. Saminadayar, Phys. Rev. Lett. **90**, 056801 (2003).
[4] P. G. N. de Vegvar, L. P. Levy, and T. A. Fulton, Phys. Rev. Lett. **66**, 2380 (1991).
[5] D. Carpentier and É. Orignac, Phys. Rev. Lett. **100**, 057207 (2008).
[6] F. Mallet *et al.*, Phys. Rev. Lett. **97**, 226804 (2006).
[7] T. Capron, Y. Niimi, F. Mallet, Y. Baines, D. Mailly, F.-Y. Lo, A. Melnikov, A. D. Wieck, L. Saminadayar, and C. Bäuerle, Phys. Rev. B **77**, 033102(R) (2008).
[8] L. Hoines, R. Stubi, R. Loloee, J. A. Cowen, and J. Bass, Phys. Rev. Lett. **66**, 1224 (1991).
[9] L. A. Fernandez, V. Martin-Mayor, S. Perez-Gaviro, A. Tarancon, and A. P. Young, Phys. Rev. B **80**, 024422 (2009).
[10] T. Capron, A. Perrat-Mabilon, C. Peaucelle, T. Meunier, D. Carpentier, L. P. Lévy, C. Bäuerle, and L. Saminadayar, Europhys. Lett. **93**, 27 001 (2011).
[11] A. B. Zorin, Rev. Sci. Instrum. **66**, 4296 (1995).
[12] D. C. Glattli, P. Jacques, A. Kumar, P. Pari, and L. Saminadayar, J. Appl. Phys. **81**, 7350 (1997).
[13] S. Mandal, T. Bautze, R. Blinder, T. Meunier, L. Saminadayar, and C. Bauerle, Rev. Sci. Instrum. **82**, 024704 (2011).
[14] O. Laborde and P. Radhakrishna, Solid State Commun. **9**, 701 (1971).
[15] J. A. Mydosh, P. Ford, M. Kawatra, and T. Whall, Phys. Rev. B **10**, 2845 (1974).
[16] U. Larsen, Phys. Rev. B **14**, 4356 (1976).
[17] D. Petit, L. Fruchter, and I. A. Campbell, Phys. Rev. Lett. **88**, 207206 (2002).
[18] D. Imagawa and H. Kawamura, J. Phys. Soc. Jpn. **71**, 127 (2002).
[19] É. Akkermans and G. Montambaux, *Mesoscopic Physics of Electrons and Photons* (Cambridge University Press, Cambridge, England, 2007).
[20] J. J. Smit, G. J. Nieuwenhuys, and L. J. de Jongh, Solid State Commun. **31**, 265 (1979).

[21] T. A. Costi *et al.*, Phys. Rev. Lett. **102**, 056802 (2009).
[22] S. Boettcher, H. G Katzgraber, and D. Sherrington, J. Phys. A **41**, 324007 (2008).
[23] L. Saminadayar, P. Mohanty, R. A. Webb, P. Degiovanni, and C. Bäuerle, Physica (Amsterdam) **40E**, 12 (2007).
[24] C. Baüerle, F. Mallet, F. Schopfer, D. Mailly, G. Eska, and L. Saminadayar, Phys. Rev. Lett. **95**, 266805 (2005).
[25] M. G. Vavilov and L. I. Glazman, Phys. Rev. B **67**, 115310 (2003).
[26] B. L. Altshuler and A. G. Aronov, in *Electron-Electron Interactions in Disordered Systems*, edited by A. L. Efros and M. Pollak (North-Holland, Amsterdam, 1985).
[27] M. Mézard, G. Parisi, N. Sourlas, G. Toulouse, and M. Virasoro, Phys. Rev. Lett. **52**, 1156 (1984).